Self-compression of loosely focused pulses in gases with power close to self-focusing critical value

Xiaowei Chen (陈晓伟), Zhinan Zeng (曾志男), Jun Liu (刘 军), Jun Dai (戴 军), Xiaofang Li (李小芳), Ruxin Li (李儒新), and Zhizhan Xu (徐至展)

State Key Laboratory of High Field Laser Physics, Shanghai Institute of Optics and Fine Mechanics, Chinese Academy of Sciences, Shanghai 201800

It is observed that the pulse duration of loosely focused pulses is self-compressed during the nonlinear propagation in argon when the input pulse peak power is close to the threshold power for self-focusing, and the results are confirmed by the numerical simulation. From the simulation we find that, near the lens focus the central part of the beam moves forward to the outer part owing to the plasma generation, and produces a leading peak in the temporal profile. And then, with the decrease of the plasma density, the spatio-temporal focusing and self-steepening effects predominate and promote a shock beam structure with a steep trailing edge. It is also found that, for our calculation case with the input pulse power close to the critical value of self-focusing, group velocity dispersion and multiphoton absorption effect have little influence on the propagation process, but the spatio-temporal focusing and self-steepening effects play a significant role in promoting the final pulse shortening.

OCIS codes: 190.5940, 190.7110, 320.5520.

Intense femtosecond laser pulses can induce complicated nonlinear changes to the refraction index of the medium, resulting in strong spatiotemporal modifications on the pulses[1,2]. Therefore the propagation of intense ultrashort pulses in a nonlinear medium attracted a lot of attention over the past decade. Especially due to its possible applications, such as optical pulse compression, lightning control and remote sensing, many studies on propagation of femtosecond pulses have been carried out experimentally and theoretically[3−9]. For laser pulses with power above the critical power $P_{\rm cr}$ for self-focusing, the beam can be compressed in space due to the third-order nonlinear susceptibility, resulting in a corresponding increase of the pulse intensity. Multiphoton ionization (MPI) occurs when the beam intensity is high enough, and the induced plasma acts as a regulating mechanism to limit the beam intensity. Thereby the formation of filamentation results from the dynamic equilibrium process of two physical mechanisms: self-focusing by the Kerr effect and defocusing by MPI. Recently it is theoretically investigated that filamentation propagation of intense femtosecond laser pulses in solid[10,11] or gas[12−15] media can lead to a remarkable pulse self-compression, with the pulse duration even to a few optical cycles. In gas medium for instance, when only diffraction, Kerr effect and MPI are considered, a 170-fs laser pulse with input power $P_{\rm in} = 1.25P_{\rm cr}$ evolves to a solitonlike structure over a long distance in the air, and the temporal profile shrinks to a single leading peak. The MPI is considered as a key mechanism for this result[13]. Moreover, it is shown that, with high input power ($P_{\rm in} > 10P_{\rm cr}$) a loosely focused Gaussian pulse beam can finally evolve into a single isolated pulse after a complex multi-peaked structure[14]. Couairon *et al.*[15] proposed a more efficient pulse self-compression scheme by filamentation in a gas with a pressure gradient. However an appropriate density profile of the gas is not so easy to achieve. So far, there have been some experiments that demonstrate the pulse self-compression in solid[16] and gas[17] materials. For example in the work of Stibenz *et al.*[17], a self-compression of few-millijoule pulses from 45 fs down to shorter than 10 fs was achieved by a filamentation in gases. It was considered that, for high-energy pulses low gas pressure for filament formation may be an important reason for the realization of the pulse self-compression, because lower value of dispersion could prevent the breakup of the soliton structure and keep an isolated short pulse during the propagation. In all the studies mentioned above, the peak power of the input pulses is much above $P_{\rm cr}$ and filamentation forms generally. However, there are few studies on the propagation dynamics with input pulse power close to the critical power.

In this paper, we investigate both experimentally and theoretically the propagation dynamics of loosely focused femtosecond pulses in argon with the power close to the threshold for self-focusing. In the experiment, the pulse duration shows an obvious self-compression, and the results are confirmed by the numerical simulation. It is revealed from the simulation calculation that the spatio-temporal distribution of the beam intensity undergoes a great reshaping. Before the focus the MPI effect predominates, and the induced plasma pushes the central part of the beam forward to the outer part and defocuses the trailing edge at the same time. While after the focus the spatio-temporal focusing and self-steepening effects predominate with the decrease of the plasma density, and promote a shock beam structure with a steep trailing edge. Finally the influence of different physical mechanisms such as group velocity dispersion (GVD), multiphoton absorption (MPA) as well as spatio-temporal focusing and self-steepening effects is discussed.

In our experiment, a commercial chirped-pulse-amplified Ti:sapphire laser system (Spectral-Physics Spitfire_50 fs) running at 1-kHz repetition rate is used as the laser source. The pulses duration is ∼50 fs with the energy of ∼0.7 mJ/pulse and the central wavelength at 800 nm. Typically, the beam quality parameter M^2 is about 1.3, and the beam diameter (at $1/e^2$ of the peak intensity) is about 7 mm. Laser pulses generated from the system is focused by a lens (focal length f=1.5 m)

into an argon-filled cell. The entrance and exit windows of the gas cell are both 1-mm-thick fused silica, and the whole length is $\sim$ 80 cm. The geometrical focus of the beam is set near the middle of the cell. After the argon-filled cell, the focused beam is collimated by a silver-coated concave mirror (f = 1 m). Then the collimated beam is separated into two parts by a thin broadband beam splitter. One small part is sent to a grating spectrometer (SpectraPro-300i, Acton Research Corporation) to monitor the spectrum, and the other part is sent to a spectral phase interferometer for direct electric-field reconstruction (SPIDER) instrument (APE Co., Ltd.) to measure the pulse temporal profile and spectral phase.

We know that, the nonlinear refraction index and self-focusing critical power of the argon are proportional to the gas pressure. Then by changing the gas pressure the ratio $P_{\rm in}/P_{\rm cr}$ can be easily controlled, which intuitively responses the strength of the self-focusing effect. In the experiment, we vacuumized the gas cell at first, and added argon slowly to increase the gas pressure, and characterize the transmitted pulses under different gas pressures. Through the nonlinear propagation in the argon-filled cell, the spatiotemporal characteristics of the laser pulse will be greatly modified, and nonlinear effects can generate new frequency components as well as a redistribution of spectrum.

When the gas cell was vacuumized, we measured the temporal profile of the transmitted laser pulses after the cell. It was found that, with the input pulse energy about 0.52 mJ the pulse duration is self-shortened from the original 53 to 41 fs. At the same time, the spectrum shows a small broadening. This is because the pulse power on the entrance window of the gas cell is high enough to induce nonlinear effects in the thin fused silica window, which can result in so-called pulse self-compression in transparent normally dispersive solid medium, which has been demonstrated by our former experiments[16]. Then we slowly added argon into the gas cell, and measured the pulse temporal profile and spectral phase at different gas pressure by using SPIDER. With the increase of the gas pressure, it was observed that the resulted pulse duration showed a decreasing trend, and the shortest pulse reached 29 fs at the argon pressure $p = 850$ mbar. Then the pulse duration keeps about 30 fs from p = 850 to 1250 mbar, and the spectrum changes little too. However, when the argon pressure is above 1250 mbar, the pulse temporal profile turns to be a multi-peak structure. The self-compressed pulse duration as a function of gas pressure is shown in Fig. 1. Moreover, the measured temporal profile, spectrum and spectral phase of the self-compressed pulses at p = 850 and 1012 mbar are given in Fig. 2. From Fig. 2 we can see that, there has no obvious original positive or negative chirp in the input pulses. And the resulted pulse is rather clear, just with some small wings. Compared with the driving pulses, the spectrum of the resulted pulses broadens more towards the blue band than towards the red band, which corresponds to the little steep falling edge of the pulse temporal profile. This results from the space-time focusing and self-steepening effects during the propagation in the argon. As for argon, the nonlinear refraction index is typically $n_2 = 9.8 \times 10^{-24} p$ (m^2/(W·atm)), and the threshold for self-focusing is $P_{\rm cr} = \lambda_0/2\pi n_2$. Then, for our experimental parameters, the corresponding $P_{\rm in}/P_{\rm cr}$ is near to 1. That is to say, the self-focusing effect is weak during the pulse propagation in the argon cell. Compared with the former experiment reporting pulse self-compression in argon[18] we find that, though the driving pulse parameters and gas pressure we used are different, the corresponding $P_{\rm in}/P_{\rm cr}$ is comparable. In their experiments, pulse self-compression was observed at an argon pressure range of $6-14$ atm, with the driving pulse is 150 fs, $\sim$ 1 mJ. Note that the driving pulse duration was extended from 150 to $\sim$ 240 fs in their experiments, the corresponding $P_{\rm in}/P_{\rm cr}$ is in the range of $0.44-1.017$. It had been qualitatively analyzed that the self-focusing effect and high-order susceptibilities were the main reasons resulting in pulse self-compression. However, more explicit analyses are needed.

In order to study the main physical mechanisms contributing to the pulse self-compression, we carried out numerical simulations for comparison with the above experimental results. The theoretical model for pulse propagation in the argon is based on the extended nonlinear Schrödinger (NLS) equation[12], coupled with the density of electrons produced mainly by multiphoton ionization (MPI). This approach has been demonstrated to be valid down to the single-cycle limit, and can accurately describe nonlinear propagation of femtosecond pulses in

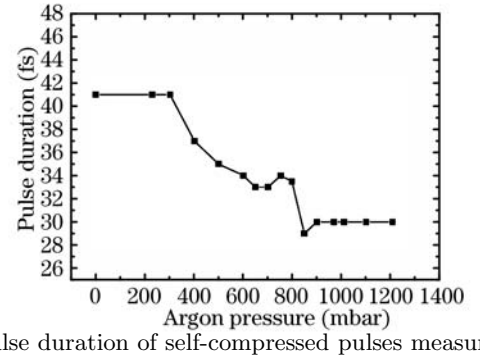

Fig. 1. Pulse duration of self-compressed pulses measured by SPIDER as a function of gas pressure of argon. The original pulse duration is $\sim$ 53 fs with the input energy $\sim$ 0.52 mJ.

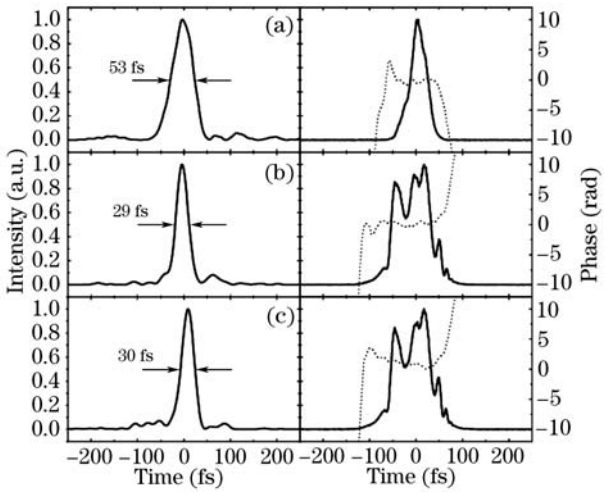

Fig. 2. Measured temporal profile, spectrum and spectral phase of the (a) original pulse and (b, c) self-compressed pulses at (b) $p = 850$ and (c) 1012 mbar.

gaseous and condensed media. In the calculation, we have considered the following physical effects: diffraction, group velocity dispersion, self-focusing, self-steepening, space-time focusing, MPI and MPA. The calculation parameters are the same as those in the experiment. The input field is considered as a Gaussian beam focused by an $f = 1.5$ m lens, with the pulse duration of 50 fs and the pulse energy of 0.52 mJ, corresponding to a peak power of 10.4 GW.

We first consider the case of $p = 850$ mbar, which corresponds to $P_{\rm in}/P_{\rm cr} \approx 0.85$. Figure 3 shows the peak intensity as a function of propagation distance in the argon, in which the lens focal point is considered as the zero position. The highest peak intensity is about 1.38×10^{14} W/cm^2. From Fig. 3 we can see that, because of the weak self-focusing effect, there is no obvious filamentation. However, due to the help of the focusing optics, the pulse peak intensity still can overturn the ionization threshold of the argon before the lens focal point. Figures 4(a) and (b) respectively show the calculated on-axis temporal and spectral profiles of the pulse at two different propagation distances. The plasma excited by MPI defocuses the trailing part of the pulse, and leads to an obvious shortening of the pulse duration (dotted line in Fig. 4(a)). But in the further propagation, because of the nonlinear dissipation of MPI after the lens focal point, this leading edge slowly disperses with giving rise to a trailing peak resulted from the effect of space-time focusing and self-steepening (solid line in Fig. 4(a)). The full width at half maximum (FWHM) duration of this trailing peak is ~ 28 fs. At the same time, the corresponding spectrum is greatly broadened and evolves from the feature of red shifting (dotted line in Fig. 4(b)) to blue shifting (solid line in Fig. 4(b)). It can be seen that, the calculated spectral profile with a blue pedestal shows a strong agreement with the experimental spectrum (Fig. 2(b)).

To illustrate the propagation process more clearly, the spatio-temporal dynamics at different propagation distances are displayed in Fig. 5. At the distance of $z = 0$ cm, owing to the plasma generation the central part of the beam moves forward to the outer part and produces a leading peak in the temporal profile. Then with the decrease of the plasma density, the spatio-temporal focusing and self-steepening effects predominate and push the pulse peak rearward, and finally promote a shock beam structure with a steep trailing edge.

We have also carried out simulations at different argon pressures. It is found that, when the peak power of the input pulse is higher, the trailing edge of the resulted pulse becomes steeper, and the former part of the pulse begins to refocus to a small prepulse. Figure 6 illustrates the spatio-temporal intensity distribution at $z = 10$ cm with $p = 1$ atm.

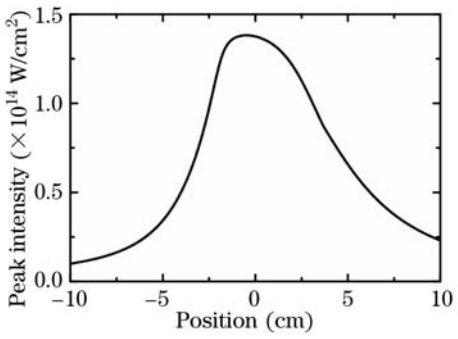

Fig. 3. Peak intensity of the pulse as a function of propagation distance.

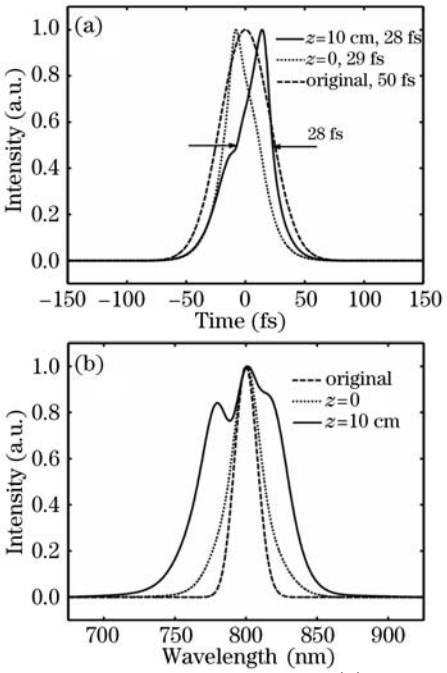

Fig. 4. Numerically calculated on-axis (a) temporal profile and (b) spectrum at $z = 0$ cm (focal point) (dotted lines) and $z = 10$ cm (solid lines) at $p = 850$ mbar, compared with those of the input pulses (dashed lines).

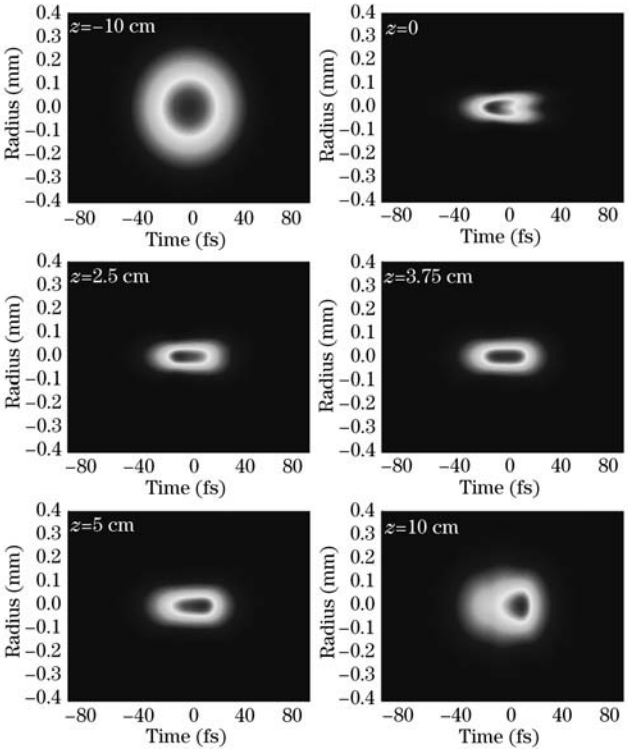

Fig. 5. Spatio-temporal dynamics at different propagation distances.

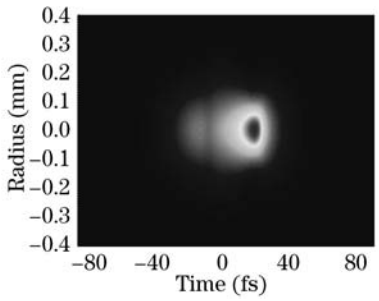

Fig. 6. Spatio-temporal intensity distribution at $z = 10$ cm with the argon pressure of 1 atm.

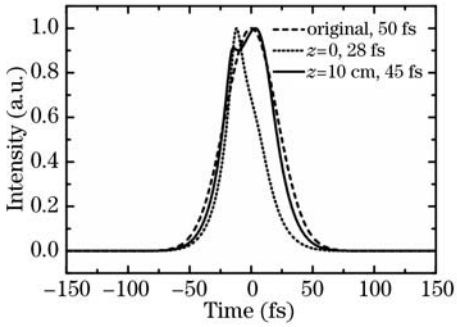

Fig. 7. Numerical calculated on-axis temporal profile at different positions at $p = 850$ mbar, compared with those of the input pulses.

In order to study the influence of the physical mechanisms, such as Kerr effect, MPA, GVD, spatio-temporal focusing and self-steepening effects, calculations are carried out under different conditions, i.e. in absence of different terms in the propagation equation. The results show that, though the effect of self-focusing is weak, it is helpful to increase the peak intensity to induce plasma, and is indispensable to the spectrum broadening of the pulse. It is also found that with the regime of $P_{\rm in}$ close to $P_{\rm cr}$, GVD and MPA have little influence on the propagation process, while the spatio-temporal focusing and self-steepening effects play a significant role in promoting the pulse shortening. Figure 7 illustrates the on-axis pulse temporal profile at different propagation distances without spatio-temporal focusing and self-steepening effects at $p = 850$ mbar. We can see that, the pulse profile at $z = 0$ cm is almost the same as the result with these two effects considered, but becomes very distinct from it after the lens focal point. Without spatio-temporal focusing and self-steepening, the pulse duration gradually broadens close to the original pulse duration at $z = 10$ cm.

In conclusion, self-compression of loosely focused femtosecond laser pulses in argon has been investigated experimentally and theoretically, with the input peak power close to the self-focusing critical threshold. The numerical simulation shows a good agreement with the experimental observations. From the calculation we find that, before the lens focal point due to the geometrical focusing optics as well as the weak pulse self-focusing effect, the pulse intensity increases high enough to induce plasma, which pushes the central part of the beam forward to the outer part and produces a leading peak in the temporal profile. And then, with the decrease of the plasma density after the lens focal point, the spatio-temporal focusing and self-steepening effects exceed the defocusing effect resulting from plasma generation and finally promote a shock beam structure with a steep trailing edge. In addition, the similar pulse self-compression was also demonstrated in the air.

This work was supported by the National Natural Science Foundation of China (No. 60578049) and the Major Basic Research Project of Shanghai Commission of Science and Technology (No. 04dz14001). X. Chen's e-mail address is fennel_chen@siom.ac.cn.

References

1. Y. R. Shen, *The Principles of Nonlinear Optics* (Wiley, New York, 1984).
2. R. W. Boyd, *Nonlinear Optics* (Academic, Boston, 1992).
3. A. Braun, G. Korn, X. Liu, D. Du, J. Squier, and G. Mourou, Opt. Lett. **20,** 73 (1995).
4. A. Chiron, B. Lamouroux, R. Lange, J.-F. Ripoche, M. Franco, B. Prade, G. Bonnaud, G. Riazuelo, and A. Mysyrowicz, Eur. Phys. J. D **6,** 383 (1999).
5. T. A. Pitt, T. S. Luk, J. K. Gruetzner, T. R. Nelson, A. McPherson, and S. M. Cameron, J. Opt. Soc. Am. B **21,** 2008 (2004).
6. A. Dubietis, G. Tamosauskas, I. Diomin, and A. Varanavicius, Opt. Lett. **28,** 1269 (2003).
7. S. Tzortzakis, L. Sudrie, M. Franco, B. Prade, and A. Mysyrowicz, Phys. Rev. Lett. **87,** 213902 (2001).
8. H. Ward and L. Bergé, Phys. Rev. Lett. **90,** 053901 (2003).
9. M. Nurhuda, A. Suda, M. Hatayama, K. Nagasaka, and K. Midorikawa, Phys. Rev. A **66,** 023811 (2002).
10. S. Henz and J. Herrmann, Phys. Rev. A **59,** 2528 (1999).
11. A. L. Gaeta, Phys. Rev. Lett. **84,** 3582 (2000).
12. S. Champeaux and L. Bergé, Phys. Rev. E **68,** 066603 (2003).
13. L. Bergé and A. Couairon, Phys. Rev. Lett. **86,** 103 (2001).
14. A. Couairon, J. Biegert, C. P. Hauri, W. Kornelis, F. W. Helbing, U. Keller, and A. Mysyrowicz, J. Mod. Opt. **53,** 75 (2006).
15. A. Couairon, M. Franco, A. Mysyrowisz, J. Biegert, and U. Keller, Opt. Lett. **30,** 2657 (2005).
16. X. Chen, Y. Leng, J. Liu, Y. Zhu, R. Li, and Z. Xu, Opt. Commun. **259,** 331 (2006).
17. G. Stibenz, N. Zhavoronkov, and G. Steinmeyer, Opt. Lett. **31,** 274 (2006).
18. I. G. Koprinkov, A. Suda, P. Wang, and K. Midorikawa, Phys. Rev. E **61,** 3847 (2000).